Theoretical Study on the Rearrangement of β-OH and γ-OH in ESI Mass Spectrometry by *N*-Phosphorylation

Zhong-Zhou Chen,† Yan-Mei Li,* Hai-Yan Wang, Jin-Tang Du, and Yu-Fen Zhao

Bioorganic Phosphorus Chemistry Laboratory, Department of Chemistry, School of Life Science and Engineering, Tsinghua University, Beijing 100084, P. R. China

Received: January 13, 2004; In Final Form: July 21, 2004

The β-OH group is more active than γ-OH in many processes, such as the catalysis of the active site in enzymes and the N→O rearrangement of *N*-phosphoryl amino acids in negative-ion electrospray ionization mass spectrometry. The pentacoordinate phosphoric intermediates are proposed and the rearrangement mechanisms are studied by ab initio and density functional calculations. The formation of the intermediates comprises a concerted route and two different stepwise pathways. The concerted route is more favored. The cleavage of the P−N bond is the rate-determining step and is favored by the proton transfer. For the rearrangement of dimethoxyl phosphoryl serine anion and homoserine anion, the activation energies are 91.2 and 156.9 kJ/mol at the B3LYP/6-31+G(d,p) level, respectively. Therefore, the β-OH group is predicted to be more active than γ-OH and the result is in good agreement with the experiments.

Serine is a conserved amino acid residue in the active sites of various enzymes.[1] In many biological processes, the side-chain β-OH group of serine plays key role in the catalytic activity. For example, many biological processes are regulated by the phosphorylation and dephosphorylation of the serine β-OH group in the proteins.[2] In most enzyme catalytic mechanisms, high-coordinate phosphoric intermediates were usually proposed as key steps.[3] *N*-phosphoryl amino acids and peptides were chemically active species that characterized the biomimic reactivities,[4,5] and it was proposed that *N*-phosphoryl amino acids were related to the phosphorylation/dephosphorylation of proteins.[6−7]

It is well known that electrospray ionization mass spectrometry (ESI-MS)[8] has been widely used for the structure elucidation in biological research. In the negative-ion ESI mass spectra of *N*-phosphoryl amino acids or *N*-phosphoryl dipeptides,[9] a characteristic rearrangement ion $(MeO)_2P(O)O^-$ was found. The ease of the rearrangement depended on the position of the side chain hydroxyl group in amino acids or peptides. The rearrangement was found in the negative-ion ESI-MS spectra of *N*-phosphoryl amino acids with a free β-OH, such as *N*-dimethyl phosphoryl (DMP) L-serine, and DMP−Thr, while those containing a free γ-OH, such as DMP−homoserine (HSer), did not have the rearrangement (Scheme 1). The arrangement was postulated by the participation of β-OH, not by γ-OH. Moreover, MNDO calculations[9] showed that the relative energy of pentacoordinate phosphoric intermediate **2** was about 40 kJ/mol lower than that of **3**. However, the semiempirical MNDO calculations do not give the overall reaction pathways and distinguish the activity difference between β-OH and γ-OH quantitatively. To study the reaction mechanism and the effect of the side chain hydroxyl group on the rearrangement precisely, further calculations are needed. It might be useful to understand the intrinsic relationships between the phosphoryl groups and the amino acid residues during the phosphorylation/dephosphorylation of proteins.

SCHEME 1. Proposed Reaction Pathways for Negative-Ion ESI−MS/MS Rearrangement of *N*-Phosphoryl Serine (1a) and Homoserine (1b)

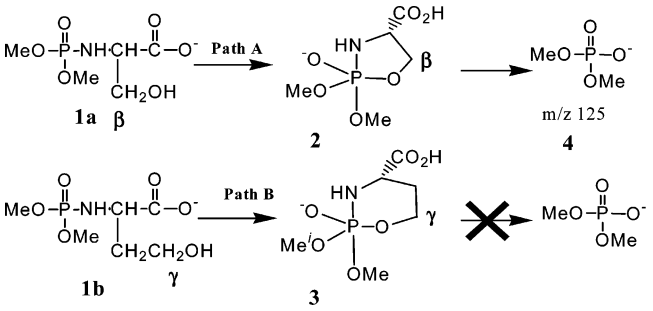

Modeling and Computational Details

N-Dimethyl phosphoryl (DMP) L-serine (**1a**) and L-homoserine (**1b**) are taken as the reactants, and the rearrangement reaction pathways are shown in Scheme 1. The geometries were optimized at the HF/6-31G(d,p) and B3LYP/6-31+G(d,p) levels, respectively.[10] The transition states were found with synchronous transit-guided quasi-Newton (STQN) methods.[11] Intrinsic reaction coordinate (IRC) calculations of the transition states were performed to confirm that the transition states were located on the real saddle points of the reaction potential energy surfaces. Natural bond orbital (NBO) analysis[12] and frequency calculations were performed for each optimized structure. Zero-point vibrational corrections and thermal corrections are considered for the energies at the B3LYP/6-31+G(d,p) level. The relative energies (RE) refer to the energies relative to the corresponding phosphoryl amino acid anion.

All quantum chemical calculations were carried out with Gaussian 98 software[13] on a Power Challenge R12000 workstation. All molecular modeling was performed on an SGI workstation with the SYBYL6.7 software package (Tripos Inc., St. Louis, MO, 2000).

* Corresponding author. Telephone: 86-10-62772259; Fax: 86-10-62781695; E-mail: liym@mail.tsinghua.edu.cn.

† Present address: National Jewish medical and research center, 1400 Jackson St., room K405, Denver, CO 80206.

10.1021/jp040024i CCC: $27.50
Published on Web 08/27/2004

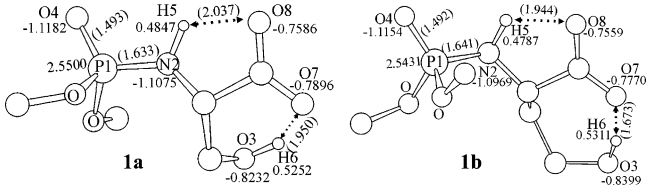

Figure 1. DMP−Ser (**1a**) and DMP−HSer (**1b**) anions optimized at the B3LYP/6-31+G(d,p) level. The NBO atomic charges and the distances (in parentheses, Å) were shown in the figures.

TABLE 1: Relative Energy (RE) of Pentacoordinate Phosphoric Intermediates at the HF/6-31G(d,p) Level

isomer[a]	RE (kJ/mol)	isomer	RE (kJ/mol)	isomer	RE (kJ/mol)
2a	138.3	**3a**	210.2	**3g**	190.0
2b	73.8	**3b**	126.4	**3h**	283.9
2c	124.5	**3c**	171.9	**3i**	286.8
2d	167.0	**3d**	228.1		
2e	107.5	**3e**	118.0		
2f	106.1	**3f**	185.9		

[a] **2** and **3** stand for intermediates containing five or six-member rings, respectively. Hydroxyl group is on the ring plane for **a**, **d**, **g**; at the same side of the rest carboxylic group for the plane for **b**, **e**, **h**; at the different side for **c**, **f**, **i**. Structures **2d**, **2e**, **3d**, **3h** and **3i** are unstable during optimization, the energies correspond to the structures in which the angle of two apical bonds is fixed at 170°.

Results and Discussions

DMP−Ser (**1a**) and DMP−HSer (**1b**), constructed according to the crystal structure of *N*-diisopropylphosphoryl (DIPP) alanine,[14] are optimized at the B3LYP/6-31+G(d,p) level with geometries shown in Figure 1. The dihedral angles of O4−P1−N2−H5 in **1a** and **1b** are in agreement with the crystal geometry of DIPP−Ala. Two hydrogen bonds between α-carboxylic anion and imide group or hydroxyl group are found, respectively. The additional CH_2 group in **1b** makes the side chain γ-OH more flexible and the formation of hydrogen bonds easier. In Figure 1, the intramolecular hydrogen bond O3−H6···O7 in **1b** is in a seven-membered ring, while it is in a six-membered ring in **1a**. Moreover, the shorter distance between O7 and H6 atoms and the larger angle O3−H6···O7 make the hydrogen bond O3−H6···O7 in **1b** stronger than that in **1a**.

From the experiments,[9] the rearrangement was postulated by the formation of the pentacoordinate phosphoric intermediates **2** and **3** (Scheme 1). Here, quantum chemical calculations are carried out to analyze the overall reaction mechanism and to compare the activity of the β-OH group in **1a** with γ-OH in **1b**.

Pentacoordinate Phosphoric Intermediates 2 and 3. Pentacoordinate phosphoric intermediates **2** from the β-OH of **1a** contain a five-membered ring, while intermediates **3** from the γ-OH of **1b** contain a six-membered ring (Scheme 1). The pentacoordinate phosphoric intermediates **2** and **3** should take trigonal bipyramidal configuration according to ref 15. So there are six positional isomers (**2a**−**2f**) for intermediates **2**, while for intermediates **3**, there are totally nine positional isomers (**3a**−**3i**), since the arrangement of six-membered ring might exist as apical-equatorial spanning (**3a**−**3f**) or diequatorial spanning (**3g**−**3i**).[15] To find which is most stable in each kind of intermediates, the fifteen isomers are optimized at the HF/6-31G(d,p) level and their relative energies are listed in Table 1. According to Table 1, the isomers **2b** and **3e** are the most stable among intermediates **2** and **3**, respectively. Isomer **3b**, most stable among isomers with the P−N bond in the equatorial position, is 8.4 kJ/mol higher than **3e**. Therefore, the pentacoordinate phosphoric intermediate anions do not prefer the isomers with P−N bond in the equatorial positions and differ greatly from the neutral intermediates.[16] Meanwhile, isomer **3g** is the most stable among intermediates **3** with six-membered ring in diequatorial spanning arrangement. For each kind of isomers, the most stable structures are those in which the oxygen anion and the carboxylic group are at the same side of the ring due to low bulkiness of the oxygen anion. In addition, the hydrogen bonds between the oxygen anion and the carboxylic group can make the isomers more stable.

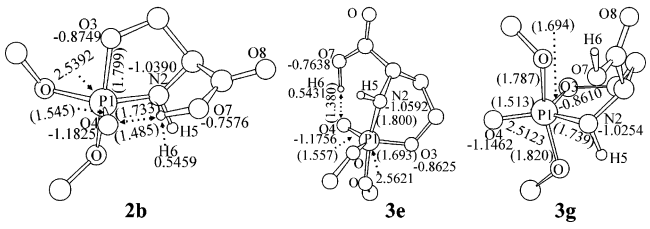

Figure 2. Geometries **2b**, **3e**, and **3g** at the B3LYP/6-31+G(d,p) level (supra note).

The optimized geometries of **2b**, **3e**, and **3g** at the B3LYP/6-31+G(d,p) level are depicted in Figure 2. Comparing isomers **3e** and **3g**, no intramolecular hydrogen bond is found in **3g**, while a strong seven-membered intramolecular hydrogen bond O4···H6−O7 exists in geometry **3e** (Figure 2). Moreover, for the larger strain with its ring at the equatorial position and the ring angle of N2−P1−O5 (106.5°) compared to the standard angle (120°) of trigonal bipyramidal configuration, the free energy of isomer **3g** is 85.7 kJ/mol higher than **3e**. The energy difference is so large that intermediates **3** should exist in the apical-equatorial arrangement. The results are consistent with the similar structures discussed in refs 15 and 16. Comparing geometries **2b** and **3e**, the relative free energy of **2b** is 48.8 kJ/mol lower than that of **3e**. The main parameters are quite different for the different type of ring. The longer P1−N2 bond makes the atoms around the phosphorus atom in **3e** more crowded than those in **2b**. Meanwhile, the absolute NBO charges of P1 and N2 atoms in **3e** are 0.0229 and 0.0202 larger than those in **2b**, respectively. It means that **3e** is more reactive than **2b**. Therefore intermediates **2** containing five-membered rings should be more stable than intermediates **3** containing six-membered rings.

Formation of Pentacoordinate Phosphoric Intermediates. To form pentacoordinate phosphoric intermediates **2** and **3**, it might comprise a concerted pathway and two different stepwise routes (Scheme 2). In the concerted route, the transfer of proton H6 from the hydroxyl group to the carboxylic anion and the formation of bond P1−O3 are cooperative in formation of the intermediates. However, the stepwise pathways consist of two steps, proton H6 transfer and bond P1−O3 formation (Figure 3 and Figure 4).

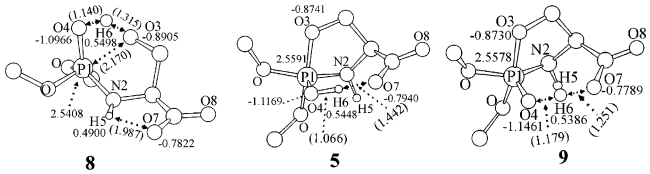

Figure 3. Geometries of the intermediate **5** and transition states **8** and **9** at the B3LYP/6-31+G(d,p) level.

For the stepwise pathway A, optimized geometries of **8**, **5**, and **9** at the B3LYP/6-31+G(d,p) level are depicted in Figure 3. The transition state **8** contains a seven-membered hydrogen-bond-bridge O4−H6···O3 structure. Transition state **8** is stable by the hydrogen bond N2−H5···O7. For the transition state **9**,

SCHEME 2. Concerted and Stepwise Pathways Involved in Forming 2b from 1a

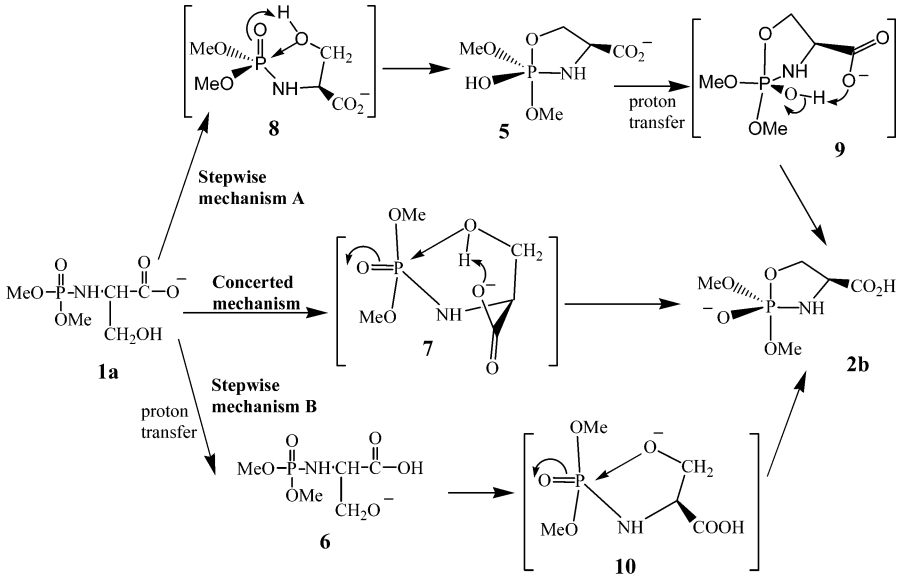

the hydrogen H6 is partially transferred to the O7 atom. From Figure 5, the formation of the intermediate **5** is the rate-determining step in the stepwise pathway A. Therefore, the overall activation energy of the stepwise pathway A is 125.6 kJ/mol at the B3LYP/6-31+G(d,p) level. For the stepwise pathway B, the optimized geometries of **6** and **10** at the B3LYP/6-31+G(d,p) level are depicted in Figure 4. The transition state **10** is corresponding to the transition state of the bond P1−O3 formation. In the intermediate **6**, the hydrogen bond N2−H5···O3 is found. Moreover, the structure **6** with a hydrogen bond O7−H6···O3 would be converted to **1a** during optimization. In the proton-transfer process, no transition state is found. Nevertheless, the overall activation energy of the stepwise pathway B is not less than 150.8 kJ/mol at the B3LYP/6-31+G(d,p) level.

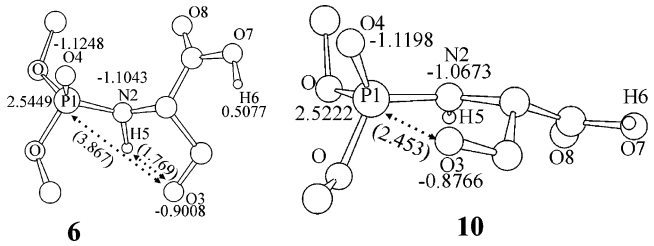

Figure 4. Geometries of the anion **6** and transition state **10** at the B3LYP/6-31+G(d,p) level.

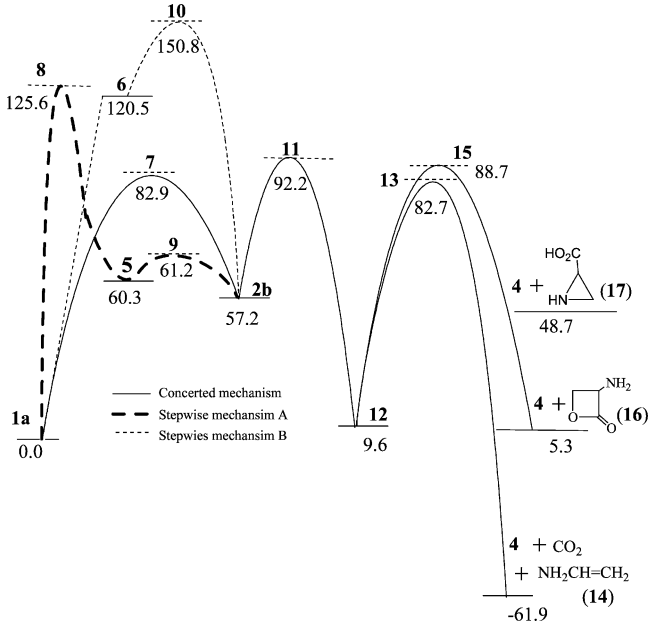

Figure 5. Energies (kJ/mol) profile for the mechanisms at the B3LYP/6-31+G(d,p) level.

With relative energy value of 82.9 kJ/mol at the B3LYP/6-31+G(d,p) level, **7** is the transition state of the concerted process. Comparing the transition states in the three processes, the NBO charges of the phosphorus atom in **8** and **10** are higher than that in **7**, making the transition states **8** and **10** more reactive. In addition, the bond P1−O3 formation is considered as the rate-determining step in both stepwise processes. The proton transfer in the concerted process (Figure 6) makes the formation of the bond P1−O3 easier. Therefore, the concerted pathway is more favored over the two stepwise processes (Table 2 and Figure 5). The three pathways involved in the formation of geometry **3e** are similar. So the formation of intermediates **2** and **3** should undergo the concerted pathway, and the proton transfer and the P1−O3 bond formation are cooperative.

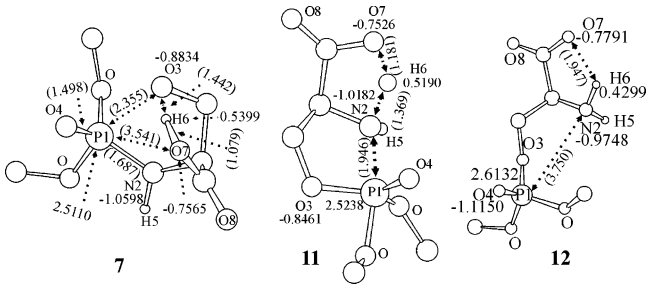

Figure 6. Transition states **7** and **11** and geometry **12** at the B3LYP/6-31+G(d,p) level.

Fragmentation of Pentacoordinate Phosphoric Intermediates. To produce the rearrangement product **4**, the P1−N2 bond in the intermediates **2b** should be cleaved. Geometry **12** is the product corresponding to the cleavage of the P1−N2 bond and **11** is the corresponding transition state (Figure 6), while the transition state directly from **1a** to **12**, with a higher relative

SCHEME 3. Three Possible Fragmentation Pathways Involved in Forming 4 from 12

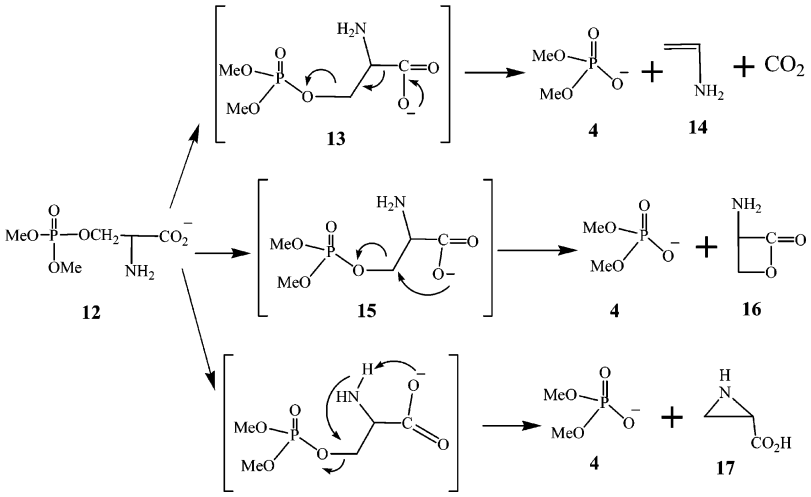

TABLE 2: Relative Energy of Key Intermediates and Transition States

RE (kJ/mol)	HF/ 6-31G(d,p)	B3LYP/ 6-31+G(d,p)	ΔH^a	ΔG^a	single-point energy[b]
2b	73.8	57.2	52.3	63.7	63.4
7	102.6	82.9	73.1	83.1	85.7
11	145.9	92.2	80.6	91.2	99.8
12	4.3	9.6	10.5	6.9	14.0
13	135.9	82.7	73.7	64.8	78.2
15	108.7	88.7	82.8	81.6	92.4
3e	118.0	98.5	93.3	112.5	102.6
3g	190.0	183.7	182.1	198.2	183.4
18	143.2	115.8	104.5	119.3	117.9
19	199.0	150.4	139.5	156.9	155.7
ΔE(3e−2b)	44.2	41.3	41.0	48.8	39.2

[a] ΔH and ΔG were calculated at the B3LYP/6-31+G(d,p) level (considering ZPE and thermal correction). [b] The single-point energy was calculated at the B3LYP/6-311+G(d,p)//B3LYP/6-31+G(d,p) level (not considering any correction).

energy value of 226.0 kJ/mol at the B3LYP/6-31+G(d,p) level, is not favored. Figure 5 shows that the cleavage of the P1−N2 bond is the rate-determining step. For the transition state **11**, proton H6 is partially transferred from O7 atom to N2 atom and it promotes the cleavage of the P1−N2 bond. The cleavage of the P1−N2 bond in **3e** is similar.

There are three possible products from **12** (Scheme 3). Except for **4**, the other products might be carbon dioxide and vinylamine (**14**), four-membered ring product (**16**), or three-membered ring product (**17**). Because the neutral compounds cannot be detected by mass spectrometry, it is necessary to compare the three pathways. In Table 2 and Figure 5, the relative energy of the three-membered ring product **17** is 43.4 kJ/mol higher than **16** at the B3LYP/6-31+G(d,p) level and the relative energy of forming the three-membered ring product (**17**) is 191.0 kJ/mol higher than **11** at the HF/6-31G(d,p) level. Therefore, it is impossible to get the three-membered ring product (**17**). The chain product (CO_2 and **14**) is more stable than the four-membered ring product (**16**). To avoid the basis set superposition error, the energy of the products (**16** and **4**; **4**, **CO_2**, and **14**) are calculated as a complex, and the result is shown in Figure 5. From Figure 5, the chain product (**4**, CO_2, and **14**) is also more stable than the ring product (**4** and **16**). Therefore, the chain product is more favored thermodynamically. **13** and **15** (Figure 7) are the corresponding transition states of the chain product and four-membered ring product, respectively. **13** is more stable than **15** at the B3LYP/6-31+G(d,p) level (Table 2). So the process of producing four-membered ring product (**16**) is not favored kinetically. Therefore, the products of the rearrangement are predicted to be **4**, CO_2, and **14**, thermodynamically and kinetically. It is similar to the mechanism for the loss of C-terminal residue from protonated peptides in MALDI−PSD−MS and ESI−CAD−MS/MS.[17] The fragmentation pathway of **3e** is similar.

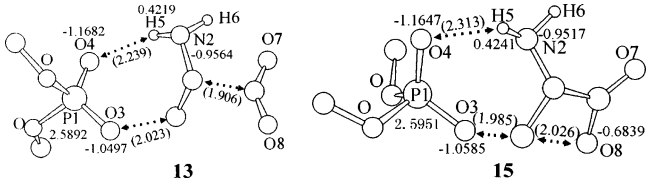

Figure 7. Transition states **13** and **15** at the B3LYP/6-31+G(d,p) level.

Difference between the Rearrangement of Phosphoryl Serine and Homoserine. The transition states **18** and **19**, corresponding to the formation and the cleavage of the P1−N2 bond of **3e**, are shown in Figure 8 at the B3LYP/6-31+G(d,p) level. In the frequency calculations, **7**, **11**, **13**, **15**, **18**, and **19** each have only one imaginary frequency at 158.46i, 998.07i, 294.94i, 472.07i, 353.33i, and 862.72i cm^{-1}, respectively. The vibrational modes corresponding to the imaginary vibrational frequencies and the IRC calculations show that the optimized structures are the corresponding transition states.

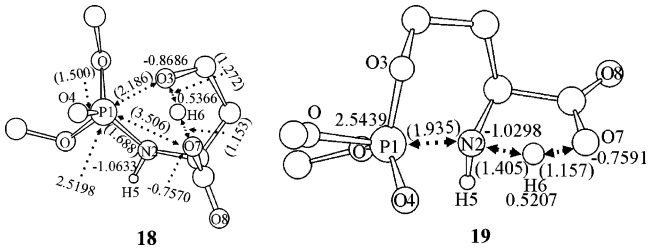

Figure 8. Transition states **18** and **19** at the B3LYP/6-31+G(d,p) level.

According to Figure 6 and Figure 8, the corresponding transition states of **2b** and **3e** differ greatly in geometric parameters. The distance between N2 and H6 atom in **11** is shorter than that in **19**. From the NBO bond analysis, the occupancy of the bond O7−H6 in **11** is less than that in **19**. So the cleavage of the bond P1−N2 in **11** is easier than **19**. In addition, the NBO absolute atomic charges of P1 and N2 in **19** are 0.0201 and 0.0116 larger than those in **11**, respectively. These make transition state **19** more active. The interactions between the lone pair electron of N2 and antibond O7−H6 σ^*

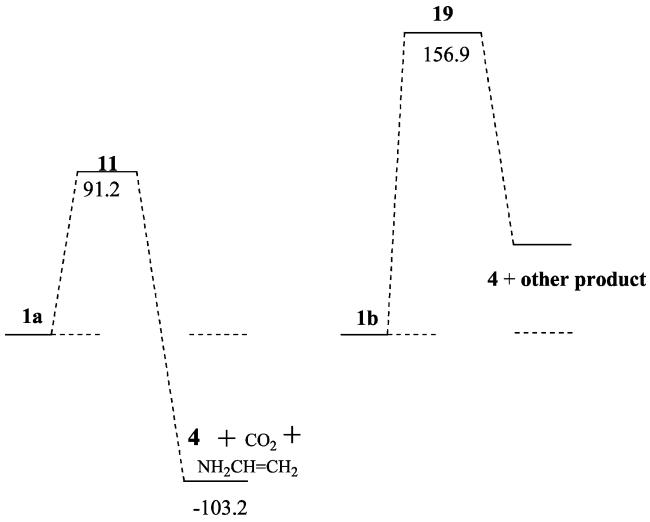

Figure 9. Relative free energy (ΔG, kJ/mol) profile for the proposed mechanisms at the B3LYP/6-31+G(d,p) level.

and the lone pair electron of O4 and antibond P1−N2 σ^* in **11** are 447.6 and 44.3 kJ/mol, respectively. The corresponding values are 388.0 and 37.6 kJ/mol, respectively, in **19**. It means that the formation of transition state **11** is easier than **19**. As a result, **11** is 65.7 kJ/mol in relative free energy lower than **19** (Figure 9). Meanwhile, the low energy value of **11** shows that the rearrangement would happen at room temperature.[18]

Therefore, the results show that the activity of the β-OH group is higher than that of γ-OH by *N*-phosphorylation. And the rearrangement ion $(MeO)_2P(O)O^-$ is found in the negative-ion ESI mass spectra of *N*-phosphoryl amino acids with a free β-OH group in the side chain, not in those with a free γ-OH group.[9] The calculations can also explain the previous experiments,[19] such as the greatly higher activity of the β-OH in phosphoryl serine than the γ-OH in phosphoryl homoserine, in processes such as N→O migration reactions, formation of peptides, and cyclophosphoroamidate and pentacoordinate phosphoric compounds.

Conclusion

For the pentacoordinate phosphoric anions **2** and **3**, the intramolecular hydrogen bond between the P−O anion and the carboxylic group, rather than the position of P−N bond, is the key to the relative order of the isomers. It is predicted that the formation of the intermediates **2** and **3** follow the concerted pathway, rather than the stepwise pathways. The cleavage of bond P1−N2 is the rate-determining step of the rearrangement and the proton transfer can decrease the activation energy. For DMP−Ser (**1a**), the products of rearrangement are predicted to be **4**, CO_2, and **14** thermodynamically and kinetically. Moreover, the activity of the β-OH group is higher than that of γ-OH by *N*-phosphorylation. The low activation energy of *N*-phosphoryl serine anion means that the rearrangement can happen under mild conditions. It can explain many experiments, such as the rearrangement of *N*-phosphoryl amino acids with a free β-hydroxyl group in the negative-ion ESI mass spectra and the formation of pentacoordinate phosphoric compounds.

Acknowledgment. We are thankful for financial support from the the Chinese National Natural Science Foundation (No. 20072023 and 20320130046), the Teaching and Research Award Program for Outstanding Young Teachers in Higher Education Institutions of MOE, P.R.C. and Tsinghua University.

Supporting Information Available: Appendices of structures and data for structures discussed. This material is available free of charge via the Internet at http://pubs.acs.org.

References and Notes

(1) Nardini, M.; Dijkstra, B. W. *Curr. Opin. Struct. Biol*. **1999**, *9*, 732.
(2) (a) Sjaastad, M. D.; Nelson, W. J. *Bioessays* **1997**, *19*, 47. (b) Yan, J. X.; Packer, N. H.; Gooley, A. A.; Williams, K. L. *J. Chromatogr. A* **1998**, *808*, 23.
(3) (a) Lee, Y. H.; Ogata, C.; Pflugrath, J. W.; Levitt, D. G.; Sarma, R.; Banaszak, L. J.; Pilkis, S. J. *Biochem.* **1996**, 35, 6010. (b) Bernstein, B. E.; Michels, P. A.; Hol, W. G. *Nature* **1997**, *385*, 275.
(4) Xue, C. B.; Yin, Y. W.; Zhao, Y. F. *Tetrahedron Lett.* **1988**, *29*, 1145.
(5) Ma, X. B.; Zhao, Y. F. *J. Org. Chem.* **1989**, *54*, 4005.
(6) Zhao, Y. F.; Cao, P. S. *J. Biolog. Phy*. **1994**, *20*, 283.
(7) Chen, Z. Z.; Tan, B.; Li, Y. M.; Zhao, Y. F.; Tong, Y. F.; Wang, J. F. *J. Org. Chem.* **2003**, *68*, 4052.
(8) Bauer, M. D.; Sun, Y.; Wang, F. *J. Protein Chem.* **1999**, *18*, 337.
(9) Chen, Z. Z.; Chen, S. B.; Chen, Y.; Li, Y. M.; Chen, J.; Zhao, Y. F. *Rapid Commun. Mass Spectrom.* **2002**, *16*, 790.
(10) (a) Becke, A. D. *J. Chem. Phys.* **1993**, *98*, 5648. (b) Wu, Y. D.; Lai, D. K. W. *J. Am. Chem. Soc.* **1995**, *117*, 11327.
(11) Peng, C.; Ayala, P. Y.; Schlegel, H. B.; Frisch, M. J. *J. Comput. Chem.* **1996**, *17*, 49.
(12) Glendening, E. D.; Reed, A. E.; Carpenter, J. E.; Weinhold, F. *NBO*, Version 3.1.
(13) Frisch, M. J.; Trucks, G. W.; Schlegel, H. B.; Scuseria, G. E.; Robb, M. A.; Cheeseman, J. R.; Zakrzewski, V. G.; Montgomery, J. A.; Stratmann, R. E.; Burant, J. C.; Dapprich, S.; Millam, J. M.; Daniels, A. D.; Kudin, K. N.; Strain, M. C.; Farkas, O.; Tomasi, J.; Barone, V.; Cossi, M.; Cammi, R.; Mennucci, B.; Pomelli, C.; Adamo, C.; Clifford, S.; Ochterski, J.; Petersson, G. A.; Ayala, P. Y.; Cui, Q.; Morokuma, K.; Malick, D. K.; Rabuck, A. D.; Raghavachari, K.; Foresman, J. B.; Cioslowski, J.; Ortiz, J. V.; Baboul, A. G.; Stefanov, B. B.; Liu, G.; Liashenko, A.; Piskorz, P.; Komaromi, I.; Gomperts, R.; Martin, R. L.; Fox, D. J.; Keith, T.; Al-Laham, M. A.; Peng, C. Y.; Nanayakkara, A.; Challacombe, M.; Gill, P. M. W.; Johnson, B.; Chen, W.; Wong, M. W.; Andres, J. L.; Gonzalez, C.; Head-Gordon, M.; Replogle, E. S.; Pople, J. A. *Gaussian 98*, revision A.9; Gaussian, Inc.: Pittsburgh, PA, 1998.
(14) Xue, C. B.; Yin, Y. W.; Liu, Y. M.; Zhu, N. J.; Zhao, Y. F. *Phosphorus, Sulfur Silicon Relat. Elem.* **1989**, *42*, 149.
(15) (a) Emsley, J.; Hall, D. *The Chemistry of Phosphorus: Environmental, Organic, Inorganic, Biochemical and Spectroscopic Aspects*; Harper & Row Ltd: London, 1976; Chapter 2. (b) Chen, Z. Z.; Tan, B.; Li, Y. M.; Zhao, Y. F. *Int. J. Quantum Chem.* **2001**, *83*, 41.
(16) (a) Chen, Z. Z.; Tan, B.; Li, Y. M.; Chen, Y.; Cheng, C. M.; Zhao, Y. F. *J. Mol. Struct.-Theochem*. **2001**, *574*, 163. (b) Chen, Z. Z.; Li, Y. M.; Ma, J.; Tan, B.; Inagaki, S.; Zhao, Y. F. *J. Phy. Chem. A* **2002**, *106*, 11565.
(17) Sadagopan, N.; Watson, J. T. *J. Am. Soc. Mass. Spectrom.* **2001**, *12*, 399.
(18) Henrickson, J. B.; Cram, D. J.; Hammond, G. S. *Organic Chemistry*, 3rd ed.; McGraw-Hill: New York, 1970.
(19) Yan, Q. J.; Yin, Y. W.; Wang, Q.; Zhao, Y. F. *Chin. Chem. Lett.* **1995**, *6*, 267.